EFFECT OF EVOLVED BUBBLES OF A GAS DISSOLVED IN A LIQUID ON RESISTANCE DURING ITS FLOW IN POROUS METALS.

II. MOTION OF WATER SATURATED WITH AIR

V. A. Maiorov and L. L. Vasil'ev

UDC 532.685

Results are presented from an experimental study conducted to determine the effect of different process parameters on the amount of increase in hydraulic resistance due to the evolution of bubbles of a gas dissolved in a liquid during its flow through porous metals.

The study [1] gave a detailed description of an experimental unit and experimental and analytical methods for investigating the effect of evolved bubbles of a gas dissolved in a liquid on hydraulic resistance during its movement through permeable matrices. Here we present results and analyze the effect of different factors on the amount of increase in resistance in this process.

Changes in Saturation of Water by Dissolved Air During Flow Through a Specimen. Water was saturated with air by mixing in glass bottles and subsequent standing under atmospheric pressure at room temperature. Curve 1 in Fig. 1 was constructed for a constant concentration of dissolved air equal to the equilibrium concentration in the initial state (at point a). The water is not saturated with the parameters above curve 1, while it is supersaturated with dissolved air below curve 1.

With an increase in pressure after the pump (shown schematically by the vertical segment ab in Fig. 1), the initially saturated water becomes unsaturated, but subsequent heating bc of the water in a thermostat again increases its saturation with air due the decrease in its solubility with an increase in temperature. With the flow of the heated water through the porous specimen its temperature remains constant, while the pressure decreases — the vertical line cde. Thus, the water first reaches saturation inside the matrix (point d) and then becomes supersaturated (section de). As soon as the saturation state is reached, air bubbles may form inside the porous metal and be carried off by the flow. The rate of this process increases with an increase in local supersaturation de. In the case of flow without preheating bc, the water reaches the saturated state only on the outer surface of the specimen (at point a).

Effect of Water Temperature. At a temperature of 20°C the saturated state is reached only on the outside surface, so no bubbles are formed inside the porous metal. Altogether, the total pressure drop over the entire specimen or parts of it over a 2-day program in series 01.a-05.a and series 01.b and 10.b (see Fig. 3 in [1]) was in agreement with the corresponding results for deaerated water on the first and thrid days — the quantities π_{2-0}, π_{1-0}, π_{2-1} did not differ from unity (such as the data in Fig. 2a).

The increase in resistance on the outlet section and over the entire specimen compared to the results for deaerated water becomes noticeable with heating and subsequently becomes more pronounced as heating proceeds — there is an increase in π_{1-0}, π_{2-0} compared to unity (the data in Fig. 2b and c). At 80°C the pressure gradient on the inlet section also increases in some cases — the value of π_{2-1} significantly exceeds unity.

The increase in resistance is most pronounced at 90°C — the data in Fig. 2d and in Figs. 3 and 4. Here, the pressure gradient over the entire specimen and on individual parts of it increases by a factor of 2-3 compared to the flow of deaerated water.

Effect of Pressure at the Specimen Outlet on Process Characteristics. The results in Figs. 2 and 3 regarding an increase in the pressure drop over the specimen in the flow of

Novopolotsk Polytechnic Institute. ITMO of the Academy of Sciences of the Belorussian SSR. Translated from Inzhernerno-Fizicheskii Zhurnal, Vol. 48, No. 3, pp. 402-409, March, 1985. Original article submitted November 30, 1983.

 0022-0841/85/4803-0290$09.50

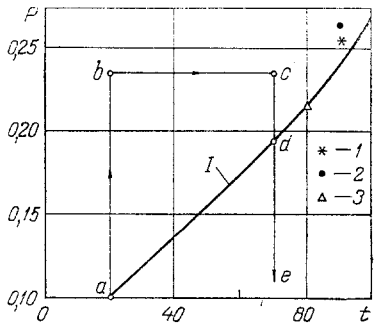

Fig. 1. Dependence of the pressure at which water is in a state of equilibrium saturation by dissolved air on temperature (water saturated at 20°C and atmospheric pressure) (curve 1). P, MPa; t, °C.

saturated water can be explained only by the effect of evolved bubbles of air dissolved in the water.

This is particularly evident from the data in Fig. 4. In series of measurements 2.12.a, with a constant flow rate G = 10 kg/(m^2·sec) and atmospheric pressure at the outlet the pressure drop over the specimen is $P_2 - P_0 = 1.12$ bar and increases by 10% over 5 min. Since the excess pressure at the outlet increases to 4.9 bar in series 2.14.a, the pressure drop decreases by a factor of 2.76 and becomes equal to the value for flow of deaerated water in series 3.12.a and 3.14.a. The absolute value $P_0 = 5.9$ bar at the specimen outlet in series 2.14.a significantly exceeds the air equilibrium saturation pressure at 90°C, which completely excludes the possibility of bubble formation.

Effect of Flow Rate. The quantity of dissolved air evolved inside the also depends on such factors as the degree of supersaturation of the liquid and the presence of bubbles in the porous structure. The number of bubbles in turn depends on the history of the process. These hard-to-predict factors also lead to a significant change in the results in Figs. 2 and 3.

As the temperature of the water increases first there is an increase in resistance π_{1-0} on the outlet section and, consequently, an increase in the overall resistance of the specimen π_{2-0} (Fig. 2b and c). Only at the temperature of 80-90°C is there an increase in resistance π_{2-1} on the inlet section (Fig. 2d, and e, and Fig. 3). Meanwhile, in every case there is a monotonic increase in resistance with a decrease in flow rate.

All of these phenomena are clearly explained by the data shown in Fig. 5. The dashed line 1 shows the water equilibrium saturation pressure at 90°C. The lines 1, 2, and 3 show a linear decrease in pressure inside the specimen with the flow of deaerated water at the rates 17.3, 13.7, and 6.8 kg/(m^2·sec) in the measurements in series 1.05.b. Curves 4, 5, and 6 show the change in pressure with the flow of air-saturated water at the same flow rates in series 2.06b. These results are tentative because each line was drawn through only three points P_2, P_1, and P_0. On the outlet section, from the intersection of these curves with the dashed line I (point z^* for curve 4) to the outer surface ($z = 1$), the pressure of the liquid is below the equilibrium saturation pressure. Meanwhile, their difference (supersaturation) is greatest at the outlet. Thus, the first bubbles are formed in this region and air dissolved in them evolves, with the formation of a two-phase flow.

As flow rate increases (curves 4, 5, and 6, respectively), there is a decrease in pressure at all points inside the specimen, an increase in the length $l - z^*$ of the supersaturation zone, and an increase in the degree of supersaturation. Thus, there is also an increase in the length of the flow region and gas content of the two-phase mixture, which in turn decrease the relative pressure gradients π_{2-0} over the specimen and π_{1-0} over the outlet section. Since the coordinate z^* of the beginning of the supersaturation zone becomes smaller than the coordinate of the needle ($z_n = 0.39$ for specimen No. 4), conditions arise for an increase in π_{2-1} on the inlet section. In the case of low flow rates (corresponding to curve 6 and below), the pressure on the inlet surface decreases to below the equilibrium saturation pressure and bubble formation becomes possible beginning at the inlet itself. In this case,

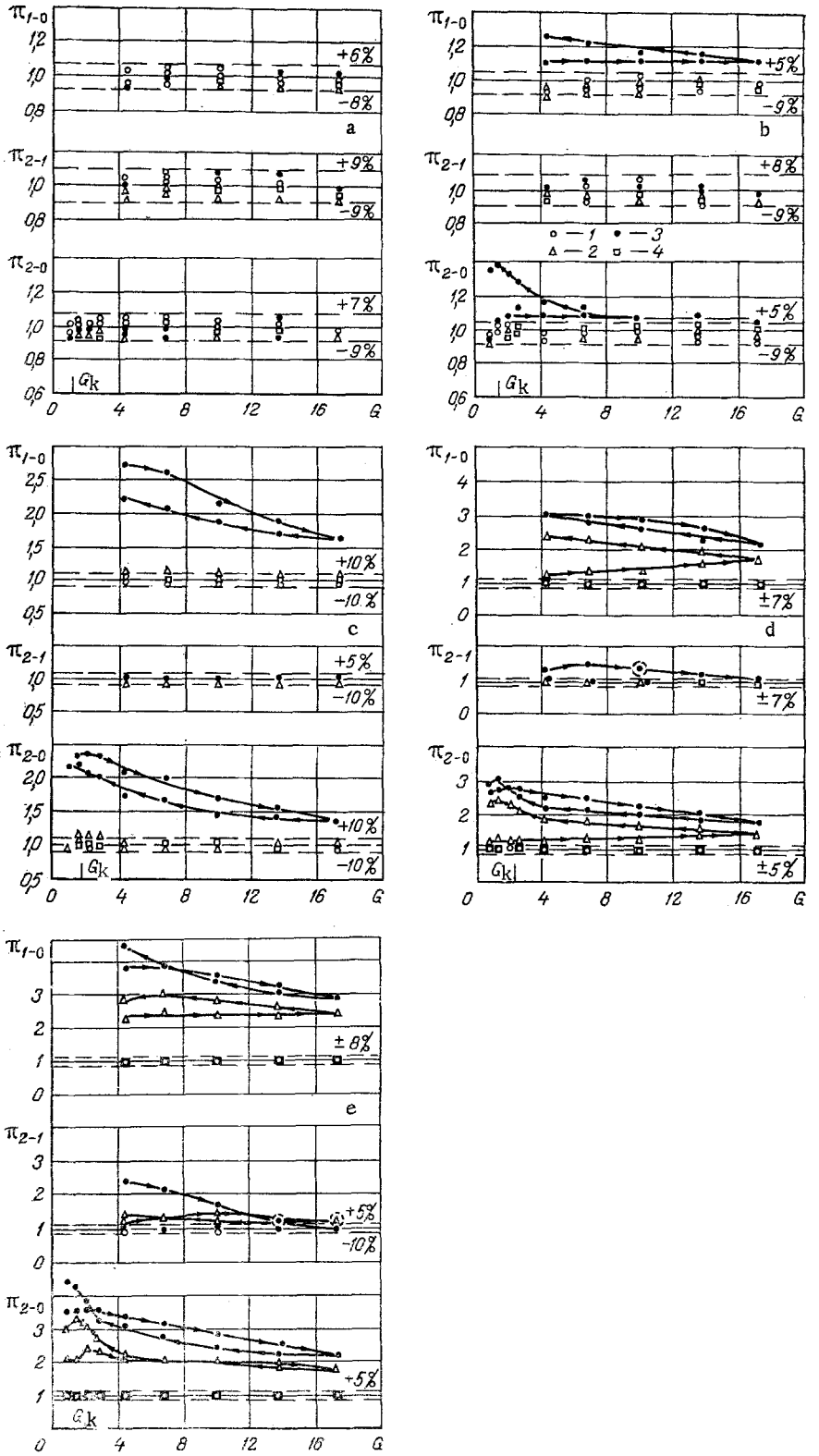

Fig. 2. Change in the relative pressure drop π_{2-0} over the entire specimen, over the section from the inlet to the needle π_{2-1}, and over the section from the needle to the outlet π_{1-0} in relation to the mass flow rate of the water G for specimen No. 4 with the following specimen temperatures in a series of measurements made by scheme "b": a) t = 20°C [1) 1.01.b; 2) 2.01.b; 3) 2.10.b; 4) 3.01.b]; b) 40 [1) 1.02.b; 2) 2.02.b; 3) 2.09.b; 4) 3.02.b]; c) 60 [1) 1.03.b; 2) 2.03.b; 3) 2.08.b; 4) 3.03.b]; d) 80 [1) 1.04.b; 2) 2.04.b; 3) 2.07.b; 4) 3.04.b]; e) t = 90°C [1) 1.05.b; 2) 2.05.b; 3) 2.06.b; 4) 3.05.b]. G, kg/m²·sec.

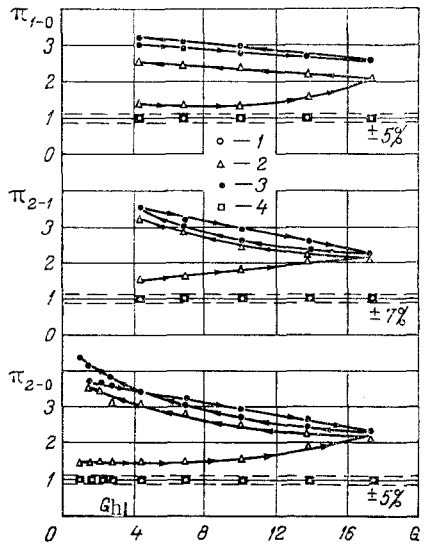

Fig. 3. Change in the quantities π_{2-0}, π_{2-1}, π_{1-0} in relation to G at a water temperature of 90°C for specimen No. 3 in the series of measurements performed by scheme "a": 1) 1.11.a; 2) 2.11.a; 3) 2.13.a; 4) 3.11.a.

there is a still greater increase in supersaturation of the liquid at all points inside the matrix, so that the amount of evolved gas and, ultimately, the values of π_{1-0}, π_{2-0}, and π_{2-1} also increase.

Effect of Capillary Pressure. It follows from the data in Figs. 2 and 3 that the relative pressure drop π_{2-0} on the specimen increases particularly sharply at low flow rates, specifically, near the point G_k noted on the x axis. The value of G_k corresponds to the same flow rate for deaerated water at which the pressure gradient $P_2 - P_0$ is created on the specimen, this gradient being equal to the capillary pressure for a cylindrical channel coinciding in diameter with the mean size d_p of the pores: $P_2 - P_0 = \Delta P_k = 4\sigma/d_p$.

Thus, with a decrease in the pressure drop on the specimen to a value commensurate with the capillary pressure, the role of the latter increases in importance. It counteracts the pushing of air bubbles through constrictions in the pores and causes a sharp increase in resistance.

Effect of Concentration of Gaseous Nuclei (the Role of the History of the Process). The most important factor — the factor determining the rate of evolution of the dissolved gas and the consequent increase in resistance — is the presence of centers of evolution of dissolved gas, or gaseous nuclei, inside the porous structure. Since these nuclei are formed and accumulate in the permeable matrix gradually, the number of such nuclei depends to a considerable extent on the history of the process.

This was first observed in conducting experiments by scheme "a" at 90°C (Fig. 3). In the initial series of measurements 2.11.a there was a continuous increase in resistance both with an increase in flow rate (the forward branch of the series data) and with a decrease in flow rate (the reverse branch). This is explained by a continuous increase in the number of gaseous nuclei inside the porous metal as a whole, since even for the maximum flow rate G = 17.3 kg/(m^2·sec) the pressure at the specimen inlet P_2 = 0.248 MPa very slightly exceeds the equilibrium saturation pressure of 0.239 MPa.

In the next series 2.12.a, with a constant flow rate G = 10 kg/(m^2·sec) gas nuclei continue to accumulate inside the porous specimen over the course of 5 min (Fig. 4) because the pressure at all points inside the specimen, including at the inlet, is considerably less than the equilibrium saturation pressure. As a result, in the next series 2.13.a the forward and reverse branches of the data in Fig. 3 are very close and exceed the results for the reverse branch of series 2.11.a. Here the pressure drop on the specimen is 2.3-4 times greater than the analogous characteristic for the flow of deaerated water.

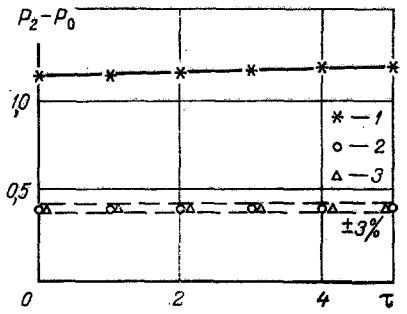

Fig. 4. Change in the pressure drop on specimen No. 3 over time with a constant mass flow rate for the water G = 10.0 kg/(m²·sec) and a temperature of 90°C in the series of measurements performed by scheme "α": 1) 2.12.a; 2) 2.14.a; 3) 3.12.a. $P_2 - P_0$, bar; τ, min.

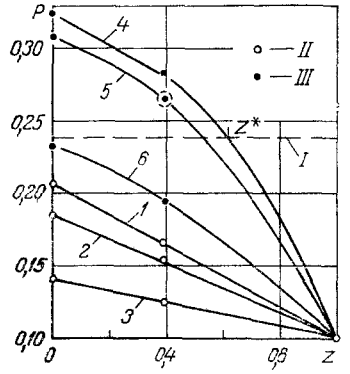

Fig. 5. Pressure drop inside specimen No. 4 during the flow of deaerated (1, 2, 3) and air-saturated water (4, 5, 6) a at 90°C with the following flow rates: 1, 4) G = 17.3 kg/(m²·sec); 2, 5) 13.7; 3, 6) 6.8 in the series: II) 1.05.b; III) 2.06.b. P, MPa.

After the removal of the gas nuclei inside the specimen in series 2.14.a, with a constant flow rate and an increased pressure at the outlet P_0 = 5 psig, the data in series 2.15.a is very close to the results of series 2.11.a, i.e., there is again a gradual accumulation of bubbles inside the porous structure.

Figure 2 shows data on measurements made according to scheme "b" (see Fig. 3 in [1]), which was devised to explain the effect of the history of the process on the rate of increase in resistance. Here, it must be noted once more that a pressure of 0.5 MPa, which considerably exceeds the equilibrium saturation pressure, was created in the intervals between the series during temperature changes in order to eliminate air bubbles in the specimen. Nevertheless, we obtained sharply differing results. Whereas the increase in resistance was very slight with a sequential increase in temperature and was seen only at low flow rates at 60°C (series 2.03.b in Fig. 2c), in the reverse process at the same temperature of 60°C it was quite substantial (series 2.08.b in Fig. 2c). Also, there was a marked increase in resistance at the lower temperature of 40°C — series 2.09.b in Fig. 2b.

An even more substantial difference was seen at 80°C (Fig. 2d). When this temperature is approached from below, there is a continuous increase in resistance both with an increase in

flow rate (the straight branch of series 2.04.b in Fig. 2d) and with its decrease (the reverse branch). This is evidence of the continuous accumulation of gas nuclei inside the porous structure, but only on the outlet section — the value of π_{2-1} on the section between the inlet and the needle remains equal to unity. When 80°C is approached from above (series 2.07.b), the forward and erverse branches of this series are close to each other (the forward being higher than the reverse) and the data significantly exceeds the data for the reverse brach of series 2.04.b. This is evidence of saturation of the permeable matrix by gas nuclei by the time series 2.07.b began, with the saturation occurring even earlier in the case of an increase in flow rate. This development is particularly evident for the section between the inlet surface of the specimen and the needle: the value of π_{2-1} is greater than unity and decreases with an increase in flow rate. With a decrease in flow rate, π_{2-1} is equal to unity. At the beginning of the series, there were gas bubbles in the inlet section. They disappeared (were wahsed away and dissolved) as flow rate increased and were not able to form again as flow rate subsequently decreases.

The difference between the data for pairs of series 02.b and 09.b, 03.b and 08.b, 04.b and 07.b, and 05.b and 06.b, obtained at the same temperatures for each pair but with opposite directions of change in temperature between measurements, shows that there is a continuous accumulation of gas nuclei in the porous material in series 02.b-06.b. Meanwhile, their presence first significantly affects resistance at 60°C. In series 06.b-09.b the permeable structure is saturated with nuclei before the measurements began. The bubbles become evident at a substantially lower temperature: 40°C. Thus, in series 2.07.b at 80°C and in series 2.08.b at 60°C, the forward branches are higher than the reverse branches (Fig. 2c and d). There naturally arises the question: from where do these bubbles appear if the pressure in the specimen during the time of the decrease in the temperature of the thermostat between series 06.b and 09.b exceeds the equilibrium saturation pressure for water containing dissolved air? It can be suggested that they are compressed within the porous matrix but do not disappear completely as pressure increases — it is known that in locating a microscopic bubble inside a contracted microscopic cavity with poorly wetted surfaces ($\Theta > \pi/2$) the gas pressure in it may be considerably less than the pressure of the liquid, and the gas nucleus is preserved.

Degree of Supersaturation with Evolution of Bubbles in a Liquid Flow Inside a Porous Metal. It is interesting to determine the level of supersaturation of water at which bubbles begin to form inside the porous structure. In connection with this, we should particularly note that for specimen No. 4 in the three series 2.05.b, 2.06.b, and 2.07.b we observed one regime. Here, the relative pressure gradient π_{2-1} in the inlet section was considerably greater than unity, while the pressure at the needle P_1 was greater than or equal to the equilibrium saturation pressure. These results are denoted by the circles in Fig. 2d and e. One of the results was also plotted in Fig. 5, and all of them are depicted by the points 1-3, respectively, in Fig. 1. The value $\pi_{2-1} > 1$ is evidence of an increase in resistance due to the presence of air bubbles on the section upstream from the needle. Thus, in these isolated cases, bubbles exist on the section from the inlet to the needle at a pressure which exceeds the equilibrium saturation pressure.

All of these findings are characterized by the fact that they were obtained in a regime of sequential increase in flow rate, when the beginning of the supersaturation region is shifted toward the outside surface of the specimen. It is evident that prior to measurement the porous structure was saturated with gas bubbles and that the latter did not completely disappear by the time of measurement in those regions where the pressure was equal to or greater than the equilibrium saturation pressure. The results also show that with a long period of flow and in the presence of numerous nuclei inside the permeable matrix, the process of bubble formation and the evolution of dissolved gas in the bubbles stabilize and proceed with a slight supersaturation of the water with dissolved air. Such conclusions are in complete accord with the data obtained in [2] in a determination of the condition under which gas bubbles begin to appear in a flow leaving a porous metal.

LITERATURE CITED

1. V. A. Maiorov and L. L. Vasil'ev, "Effect of evolved bubbles of gas dissolved in a liquid on resistance during its flow in porous metals. I. Motion of deaerated water," Inzh.-Fiz. Zh., 48, No. 2, 203-209 (1985).
2. V. A. Maiorov and L. L. Vasil'ev, "Nucleation of gas and vapor bubbles during the motion of a liquid in porous metals," Inzh.-Fiz. Zh., 42, No. 4, 533-539 (1982).